ACCESS
Arctic Climate Change
Economy and Society

Project no. 265863

ACCESS

Arctic Climate Change, Economy and Society

Instrument: Collaborative Project

Thematic Priority: Ocean.2010-1 “Quantification of climate change impacts on economic sectors in the Arctic”

D1.61 – Climate response analysis of improved model processes (sea-ice and soot) and from higher resolution

Due date of deliverable: **31/01/2015**

Actual submission date: **31/03/2015**

Start date of project: **March 1st, 2011** Duration: **48 months**

Organisation name of lead contractor for this deliverable: **Met.no**

Project co-funded by the European Commission within the Seventh Framework Programme (2007-2013)		
Dissemination Level		
PU	Public	X
PP	Restricted to other programme participants (including the Commission Services)	
RE	Restricted to a group specified by the consortium (including the Commission Services)	
CO	Confidential, only for members of the consortium (including the Commission Services)	

Contents

1 Climate model analysis and sensitivity of improved model processes (sea-ice and soot) and from higher resolution.

Jens Boldingh Debernard, Øyvind Seland, Trond Iversen, Alf Kirkevåg

Arctic climate is strongly influenced by the presence of sea ice, which insulates the warm ocean from the cold atmosphere and reflects sunlight during summer limiting warming. Sea ice is a challenge for economic activity in the Arctic Ocean, and there is a large interest in projections for changes in sea ice climate for the coming decades. Arctic sea ice has undergone rapid changes during recent decades with a reduction of summer sea ice extent of nearly 40 % since the satellite observations started (Stroeve et al., 2014), and a significant thinning of the remaining ice (Kwok et al. 2009; Laxon et al. 2013). The thinning is related to a shift from multi-year ice (MYI) to first-year ice (FYI) (Maslanik et al, 2011) giving changed properties of the remaining ice.

Reliable modelling of the Arctic climate system is important both for understanding present changes, and for projecting future conditions. Changes in climate have to be viewed in a perspective of naturally occurring internal variability. For example, regional flow regimes cause the internal climate variability to manifest itself very differently in different regions. The climate response to external forcing is likely to depend on the nature of such regimes.

Global climate models (GCMs) and earth system models (ESMs) are applied to study both the past, present, and possible future climate. Information about past and present external climate forcing as well as scenarios for its future development is then prescribed, while the models generate climate variations and response. Thus, the model results comprise various sources of internal climate variability, and responses to both natural and anthropogenic forcing, which are influenced by unavoidable uncertainties in the formulation of processes in the models.

According to the Intergovernmental Panel of Climate Change (IPCC), climate variability refers to “variations in the mean state and other statistics (such as standard deviations, the occurrence of extremes, etc.) of the climate on all spatial and temporal scales beyond that of individual weather events. Variability may be due to natural internal processes within the climate system (internal variability), or to variations in natural or anthropogenic external forcing (external variability)."

Here we deviate slightly from this terminology by replacing the term “external variability” with climate response or climate change. Thus, natural variability includes any variation in quantitative variables related to weather which occur with no net external forcing. Natural variability is caused by dynamic instabilities maintained against frictional dissipation by persistent replenishment of the entropy of the climate system. Through

interactions with the ground surface, the state of the atmosphere can switch between different apparent modes of variability. These are frequently associated with atmospheric teleconnections (Bjerknes, 1969; Hoskins and Karoly, 1981, Dawson et al., 2012).

The analysis of the NCEP re-analyses by Corti et al. (1999) indicated that observed multi-decadal climate trends, possibly influenced by a general northern hemispheric or global warming, can be associated with naturally occurring regional flow patterns. This conceptual interpretation implies that the patterns of climate response correspond to existing patterns of natural variability, provided that the external forcing is moderate (Palmer, 1999). The frequency of occurrence of these patterns may change considerably while only negligible changes in the shape of the patterns are seen. Therefore, for future predictions of climate change, including long term trends and variability in sea-ice, understanding the underlying processes responsible for the regional characteristics of internal variability is important.

This work includes studies and tests of three aspects of climate modelling using the NorESM : climate response and of soot aerosols, the representation of specific sea-ice features, and the dependence of climate simulations on spatial model resolution. These three aspects are all key to the understanding of the Arctic climate system and hence also the global. They are not specific issues for NorESM in particular, but represent common challenges to the quality of the modelling of the global climate and its response to changes that incur external forcing.

Since much of the improvements in black carbon (BC) modelling was already included in the CMIP5 version of NorESM, this topic is somewhat separated from the two others and is discussed in a separate subsection. The improvements caused by changed ice-ocean parameterisation and increased model resolution are described in separate subsections below.

These ACCESS-results are compared to the equivalent model periods prepared for CMIP5. A thorough description of NorESM and CMIP5 experiments can be found in Bentsen et al. (2013), Iversen et al. (2013) and Kirkevåg et al. (2013). As described in the ACCESS description of work, the project also contributed to the CMIP5 work and ACCESS is included in the acknowledgements in these articles.

1.1 Climate response and sensitivity analysis of BC in NorESM

Black carbon (BC), the main light-absorbing component soot, has potential to affect climate both directly by reducing the planetary albedo, more indirectly through its impact on static stability and cloudiness of the atmosphere (the semi-direct effect), and by influencing activation of cloud droplets and cloud ice particles. Except for the impact of BC on ice-nuclei, these effects are all treated in the Norwegian Earth System Model, NorESM. Modelled effects of BC on radiative forcing as well as climate response have been investigated in several peer review papers during the last two years, most of which have ACCESS acknowledgements. A PhD has been educated based on this work. Some highlights of important results are summarized below.

The vertical transport of aerosols and aerosol precursors in convective clouds is probably over-estimated in CAM4-Oslo (Kirkevåg et al., 2013), the atmospheric module of NorESM (Bentsen et al., 2013; Iversen et al., 2013), e.g. giving a positive bias in the simulated transport of BC from low to mid-latitudes into the upper troposphere in the Arctic., and therefore probably an overestimated (in the direction of heating) direct radiative forcing (Myhre et al. 2013, Samset et al. 2013).

Based on deposition rates from CAM4-Oslo (the atmospheric component of NorESM) and other AeroCom models, concentrations of BC in snow and radiative forcing by BC in snow in the Arctic (on land and sea-ice) was studied by Jiao et al. (2013). Despite the large BC concentrations at high altitudes in the Arctic, CAM4-Oslo was shown to reproduce averaged measured BC concentrations in snow well. The studied models were generally found to underestimate the concentrations in northern Russia and Norway, and to overestimate elsewhere in the Arctic. Estimated radiative forcing by BC deposited on snow in CAM4-Oslo lies very close to (just below) the AeroCom model average.

By use of idealized climate simulations carried out with NorESM (fully coupled), Sand et al. (2013a) investigated how atmospheric BC in the mid-latitudes remotely influence the Arctic climate, compared with the response to atmospheric BC located in the Arctic itself. The study found that increased BC forcing in the Arctic atmosphere reduces the surface air temperature within the Arctic, with a corresponding increase in the sea-ice fraction, despite the increased planetary absorption of sunlight. The analysis indicates that this effect is due to a combination of a weakening of the northward heat transport caused by a reduction in the meridional temperature gradient and a dimming at the surface. On the other hand, BC forcing at mid-latitudes leads to a significant

warming of the Arctic surface and a decrease in the sea-ice fraction. These results suggest that mitigation strategies for the Arctic climate should also address BC sources outside the Arctic, even if they do not contribute much to BC concentrations in the Arctic.

In another NorESM study by Sand et al (2013b), also a part of ACCESS (although failed to be mentioned in the Acknowledgment), BC from fossil fuel and biofuel combustion was estimated to yield an almost five times larger Arctic surface temperature response per unit of emitted mass when emitted within the Arctic than when emitted at mid-latitudes. This is to a large extent due to increased absorption of solar radiation when BC is deposited on snow and ice. The modelled reduction of sea-ice is particularly pronounced in late summer. To the extent that such climate model projections are reliable (see IPCC, AR5 for such discussions), a future increase in Arctic BC emissions from enhanced shipping in winter and early spring may therefore amplify the already observed decline in summer sea-ice concentrations.

In the most recent paper by Sand et al. (2014) using NorESM the climate response to an abrupt increase of black carbon (BC) aerosols is compared to the similar and standard CMIP5-experiment of quadrupling CO_2 concentrations in air. Fossil fuel BC emissions are multiplied by 25 which produces an instantaneous top-of-atmosphere radiative forcing comparable to that of the CO_2 quadrupling. The response to BC is very different from that of CO_2. Fast feedbacks act to equilibrate the increased atmospheric BC-absorption of sunlight by enhancing the outgoing longwave terrestrial radiation with only minor changes to the surface temperature (see Figure 1) and surface evaporation. Fast feedbacks are much more dominating for BC than for CO_2: changes in air temperature, clouds, and precipitation are considerable even though changes in the global mean surface temperature are modest.

Although we find considerable regional differences in surface temperature response, areas with cooling and warming tend to cancel and the net fluxes of heat between ocean an atmosphere are so small that the climatologically inert deep oceans are hardly involved. In summary, BC aerosols possess unique properties which reduce the relevance of the traditional concept of climate sensitivity as a simple relation between TOA forcing and surface temperature. Furthermore, emission-driven BC responses in the atmosphere are found to be much larger than concentration-driven, at least in NorESM, see Figure 1. This implies that prescribing BC concentrations may lead to strongly inaccurate conclusions, although other models with less efficient transport may produce results with smaller differences.

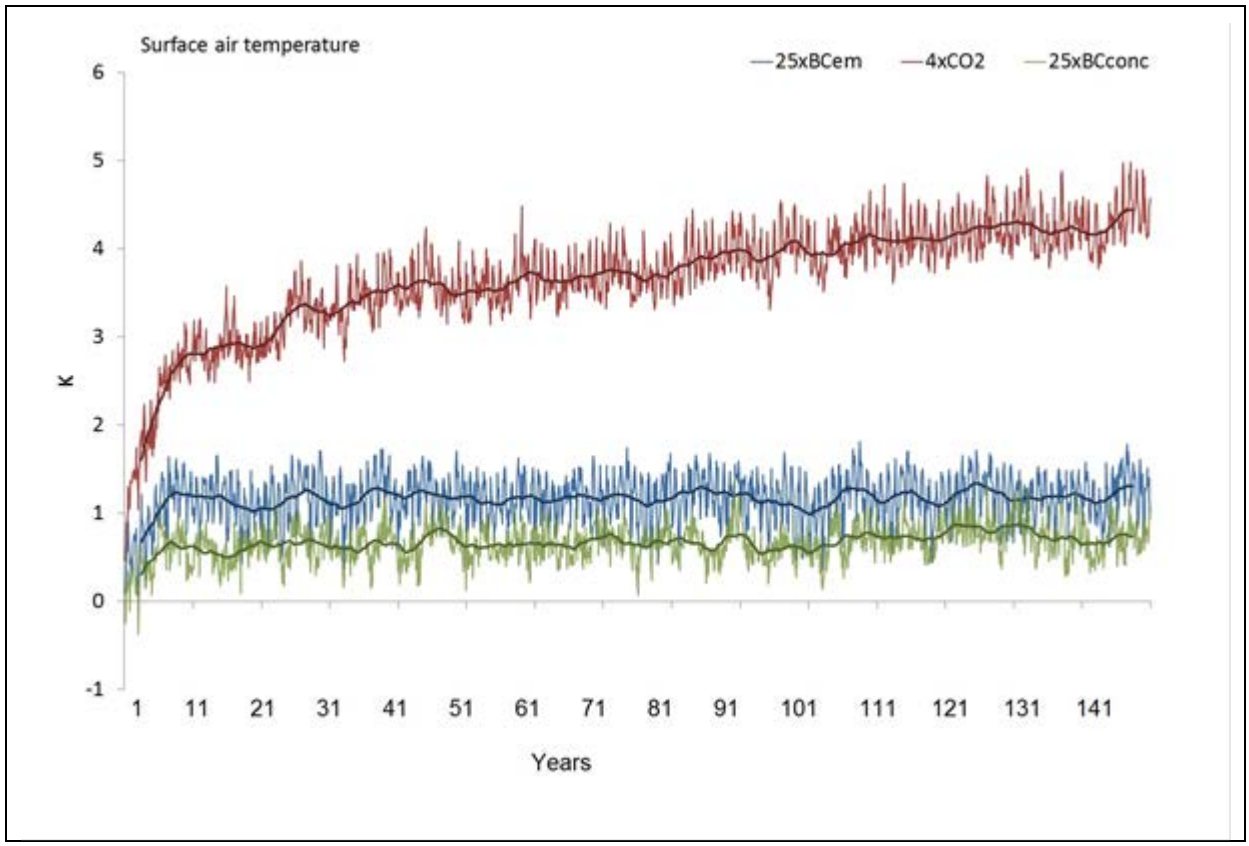

Figure 1: Global average surface temperature response (in K) for 25×BCem (emission driven, blue), 25×BCconc (concentration driven, green) and 4×CO2 (red) simulated with the fully coupled NorESM. The thick lines show 5-year running means. The tick marks on the the x-axis represent January each 10th model year. (from Sand et al., 2015).

1.2 High-resolution experiments with NorESM. -- Motivation and model set-up

From the very start of modelling of the climate system by use of General Circulation Models / Earth System Models (GCM/ESM) there has been a competition between model complexity and resolution. Ideally one would like to run the model with sufficiently fine model resolution to obtain direct quantitative answer to society on a local scale. However, the complexity of the Earth System together with the need for long simulations and ensembles require extreme computer resources, which in effect strongly limits how fine resolution we can afford. In CMIP5 the typical model horizontal resolution is 1-2 degrees, while global scale numerical weather prediction is done on a 15-50 km grid.

The most obvious improvement one expects from a higher resolution is better representation of ground-surface details (topography, coast-lines, land-use contrasts, warm and cold ocean surfaces) . However, since the internal dynamics of the atmosphere (and the oceans) do not possess any clear spectral cut-off and there are non-linear interactions across spatial scales, simulations with higher spatial resolution should potentially improve the structure and occurrence of flow systems on large and regional scales. Dawson et al. (2012) show results from experiments where a NWP model simulates the extra-tropical regional flow structures well, while the same model with coarser "climate model resolution" looses the statistically significant representation of selected flow regimes. Associated with this is the representation of extra-tropical storm track bands. It has been shown that models that manage to reproduce North Atlantic storm-tracks (Zappa et al., 2013) usually are among models with relatively high resolution, although in this case the results are not unequivocal, possibly because of variable quality of sea-surface temperatures. The most common model pattern, including the results from NorESM, was found to be a too zonal distribution of the storm tracks over the Norh Atlantic Ocean.

The standard CMIP5 production runs with NorESM were made with a mesh width of approximately 1.9x2.5 degrees in the atmosphere. From experiments published with CCSM4 runs at NCAR, USA, (Bitz et al. 2012;

Deser et al. 2012) test runs with 1 degree atmospheric resolution and prescribed SSTs ("AMIP run") showed some improvements in circulation pattern, in particular in spring and summer, although too zonal winter storm-tracks were found for all resolutions. An experiment with 0.5 degree resolution (results not shown) improved the circulation patterns even more, although again mainly in spring and summer. Cloud and convection parameterisations in CAM4 are however not optimized for this resolution, and are not recommended for longer runs with higher resolution.

Figure 2 shows the wintertime storm-track for CAM4-Oslo with 2 degrees and 1 degree resolution compared with the ERA40 reanalysis. While the pattern is still too zonal, there is more activity in the Nordic region and the Barents Sea. In the original project plans it was suggested to run NorESM for multi-decadal time-slices with double resolution in the atmosphere and land (1x1.2 degrees). However, based on these results and an increase in available computer resources since then, we could avoid choosing particular time-slice periods and instead run a short spin-up of 200 years followed by a 20th century run and a RCP8.5 scenario run until 2100.

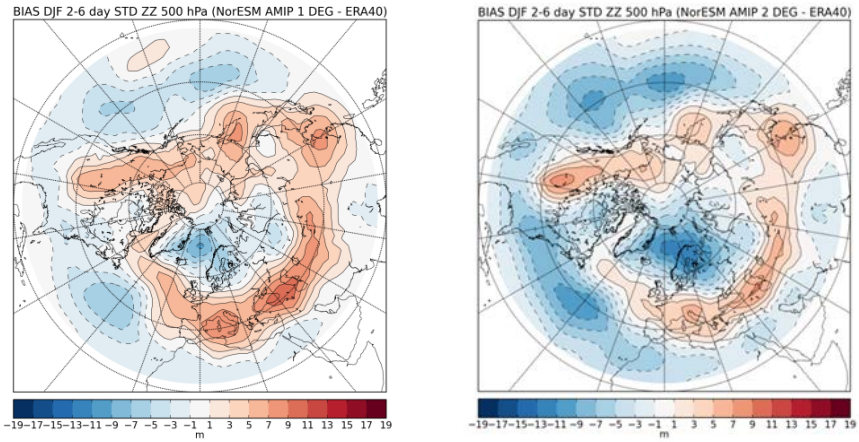

Figure 2: Winter time bias in baroclinic activity in NorESM, compared to ERA40, with the model version with 1 degree (left panel) and 2 degrees atmospheric resolution (right panel).

1.3 Sensitivity of NorESM1-M to differences in melt pond distribution on multi-year and first-year sea ice

1.3.1 Introduction

Sea ice and snow are characterized by high reflectivity to visible sunlight and have by definition a high albedo. For example a thick ice floe covered with 20 cm of cold fresh snow reflects around 87 % of the incoming visible sunlight, in stark contrast to the underlying ocean and open water leads, which reflects 7 % of the sunlight. The large differences in albedo between sea ice and snow compared with water have important consequences for the climate, and they cause strong positive sea ice – open water albedo feedbacks in ice covered regions. This means that small changes in snow and sea ice albedo can amplify and give large changes in the snow and sea ice cover, and in the amount of open water. In general, snow and sea ice have these amplifying properties when it comes to albedo and melting. Melting gives lower albedo that increase absorption of shortwave radiation and increases the melting further.

One important and decisive factor for sea ice albedo is the amount of melt water on the ice. Melt water normally collect in ponds formed in depressions at the ice surface. The size of the ponds depends on the topology of the ice surface (flat versus undulating versus deformed), the permeability of the ice, the amounts of snow and melt water. The pond albedo decreases with increasing pond depth and increases with the thickness of the underlying sea ice. This means that albedo of thick ice is higher than thin ice, and that given the same amount of melt water on the ice, shallower ponds covering larger areas lower the albedo more than deeper ponds covering a smaller surface area.

The dependences of albedo on ice thickness and melt pond distribution are important for the differences in albedo on First Year Ice (FYI) and Multi Year Ice (MYI). Normally, deformed FYI has a flat and level surface, often relatively thin, depending on the time since freezing started. In contrast, deformed MYI has survived at least one melt season, and the surface is more undulating, and in general, the ice is thick. During the start of the melting season, the ice in the Arctic is cold and impermeable, causing large fractions of melt water to stay atop of the ice and mix with snow and slush if present. The melt water will collect in depressions and cracks in the ice and form melt ponds. The difference in surface properties on MYI and FYI gives a large area fraction of shallow melt ponds on FYI, and a smaller area fraction, but deeper ponds on MYI.

Later in the melt-season, when the interior ice gets warmer, the ice gets permeable and the melt water drains down to the depth of the ocean surface. After this stage, the distributions of ponds on FYI and MYI are similar. However, due to thinner ice, and a higher absorption of sunlight during the first part of the melt season, the albedo of FYI is generally lower than that of MYI despite the similarities in melt pond distributions.

Usually, present sea ice and climate models take into account the fact that sea albedo is lower for thin ice, but only few have an explicit calculation of the amount of melt ponds. Ponds are often implicitly taken of through a reduced albedo value for bare ice, only. Also, the models do not differentiate between FYI and MYI, or their differences in melt pond distributions.

The amount of MYI has declined during the last years due to enhanced summer melting of ice, and this has caused much more FYI in the Arctic than earlier. In addition, because of the large differences in melt pond distribution and albedo on FYI and MYI it is important to investigate if the change in melt pond distribution is important for the sensitivity of the Arctic sea ice cover due to warming. The CMIP5 models as a group has slower decline in the Arctic ice extent than observed during the last decade, and there have been speculations if the sensitivity of the models would increase if they better describe the physical properties of FYI. Therefore, one of the aims with the present work is to include a parameterization of the differences in melt pond distribution of FYI and MYI into a state of the art global climate model and then check the effects of this difference on modelled climate sensitivity, both when it comes to the amount of Arctic sea ice and the global temperature response. One attempt to include the differences in melt ponds on FYI and MYI by Pedersen et al. (2009) was tested in the ECHAM5 climate model, but they had no investigation of the sensitivity of the climate response due to the parameterization.

1.3.2 Model description and parameterization of melt ponds

To investigate the impact of differences in melt pond characteristics between FYI and MYI on climate sensitivity, we have used the NorESM1-M model in a slab ocean configuration. This consists of the fully interactive NorESM1-M global climate model (Bentsen et al., 2013; Iversen et al., 2013) with the ocean component replaced by a slab ocean model (SOM). The SOM consists of a mixed layer with a depth specified from the NorESM1-M Pre-industrial (PI) control simulation delivered to CMIP5. The model has a prognostic equation for the mixed layer temperature. Temperature varies in response to varying forcing from the other model components, and to a prescribed seasonal cycle of upper ocean heat flux convergence. This heat flux convergence was calculated based on the seasonal cycles of SST and heat-fluxes to the ocean model in the PI control run from the fully coupled model. Details on the definition of the upper ocean heat flux convergence are described by Bitz et al. (2012).

In the original version, NorESM1-M uses the CICE4 sea ice model and the parameterization of melt ponds as described by Holland et al. (2012). This parameterization is modified in the present work. The model also has a prognostic variable for the relative area fraction of FYI in a grid cell. This gives a measure of the amount of FYI in the simulation, and also how this is distributed in the model. The presence of this variable allows for different treatment of melt ponds over FYI and MYI, a feature utilized here.

The melt pond parameterization of Holland et al. (2012) used in NorESM1-M has a prognostic, but rather heuristic equation for the volume of melt water on the sea ice. The volume grows if snow and ice melts, and decreases by draining to the ocean and with cold temperatures (refreezing). From the melt water volume an assumed linear relationship between the melt pond area fraction and melt pond depth is used. This relationship is based on observed ponds on MYI during SHEBA (Perovich et al., 2003):

$$A_{pf} = 1.25\, m^{-1}\, h_p$$

where A_{pf} is the melt pond area fraction of the sea ice surface, and h_p is the melt pond depth in meters. This representation and similar formulas for FYI and MYI proposed by Pedersen et al. (2009) were criticized by Polashenski et al. (2012) for not following the expected summer evolution of melt ponds on FYI. The basic problem is that the formulations do not capture the early summer phase with a large area fraction of shallow ponds. To mitigate this, we propose new equations for the relationship between area fractions and pond depths for MYI and FYI that are easy to integrate within the existing formulation of Holland et al. (2012). There are two different profiles for ponds on FYI and MYI, respectively, written in a common form:

$$A_{pf_x} = h_{p_x}(B_x e^{-\frac{h_{p_x}}{h_{m_x}}} + C_x)$$

where x denote FY or MY. Table 1 gives the values of h_{mx}, B_x and C_x. Both the new and the original formulations are shown in Figure 3 together with the formulation of Pedersen et al. (2009). Observations for MYI (SHEBA, Perovich et al., 2003) and FYI (Polashenski et al., 2012) are also shown in Figure 3. Clearly, the new equations describe shallow FYI melt pond distribution better than the original equation.

	h_m (m)	B (m^{-1})	C (m^{-1})
FY	-0.04	30	1.1
MY	-0.10	4	1.0

Table 1: Constants used in new melt pond parameterization for FYI and MYI.

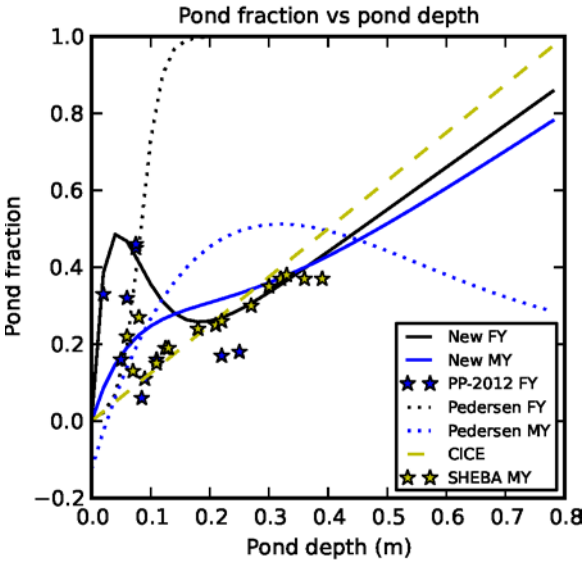

Figure 3: Melt pond area fraction as function of melt pond depth.

The variable for FYI relative area fraction is used to weight between the contributions from FYI and MYI, respectively, before shortwave absorption and albedo of the ice are calculated. To get effect of the new parameterization in CICE, we also had to do some additional adjustments. In the original melt pond scheme, inherent optical properties are interpolated between pond values and ice values for ponds shallower that 0.2 m. Unfortunately, this is in the regime with the largest differences between ponds on FYI and MYI, and the largest effects are for FYI. Therefore, we have opted to change the threshold for the interpolation such that we keep pond properties for ponds down to 0.02 m depth. For ponds shallower than 0.001 m we use bare ice optical properties.

In addition to tests with the new melt pond formulation, we made some tests with changes in snow properties that could influence the albedo and the effects of the new pond parameterization. In the present version of the model, ponds can only exist on bare sea ice, and in NorESM the fractional area of snow on the sea ice is given as

a linear equation in snow depth, up to the depth hs0 where 100 % snow cover is assumed. In the original formulation, hs0=0.03 m, a value based on measurements from the Antarctic by Brandt et al. (2005). However, this value seems low when compared with observations from the Arctic (Mauritzen et al., 2011), so we have also experiments with hs0=0.1 m. This value corresponds to a more uneven distribution of snow with larger areas of bare ice.

Evaluation of the NorESM1-M CMIP5 simulations indicates that there is too much snow during summer on the Arctic sea ice. To mitigate this problem, we have done some experiments with decreased albedo for melting snow. This is obtained by increasing the wet snow grain size to from 1500 to 2000 micrometre. In addition, the transition from dry to wet snow properties starts at a colder temperature (-2 °C compared with -1.5 °C). The effect of this "snow-tune" experiment is useful as a reference when comparing the changes with new parameterization and the increased value of hs0.

1.3.3 Climate sensitivity and set-up of experiments

One advantage of the slab-ocean model is the ability to find a near equilibrium climate in radiative balance with only a few decades of simulation time after a change of external forcing or changes in physical parameterizations. In contrast, to reach a similar type of equilibrium with a full deep ocean model would require several thousand years long simulations due to large heat capacity of the ocean. However, the transient adjustment to external forcing is not correct in the slab ocean system. Here, we utilize results for the equilibrium climate sensitivity (ECS) of NorESM1-M obtained with the slab-ocean model from experiments with doubling and quadrupling of atmospheric CO_2 concentration relative to 1850 (PI) values. These experiments give temperature increases of 3.5 deg and 7.0 deg, respectively, and they therefore agree on a ECS for the model at 3.5 degree. However, in these experiments, almost all Arctic sea ice is melted, and even the $2xCO_2$ simulation is very much warmer than present day (PD) climate, which is 0.85 degree warmer than 1880 conditions (IPCC AR5, WG1, Ch. 2). Therefore, based on the findings of the ECS we have determined the CO_2 concentration that is necessary to give an equilibrium climate around 1 deg warmer than PI-conditions the model, and thereby mimic PD conditions. The following sensitivity experiments then consist of one pair of simulations with each choice of parameterization; one simulation with PI-conditions, and one with PD-conditions. Because external forcing and CO_2 concentration are equal in all PI experiments, and similar for all PD-experiments, the difference between PI and PD climate is a measure of the sensitivity due to the actual choice of parameterization.

1.3.4 Sea ice sensitivity results from melt pond and snow experiments with slab ocean model

We summarize the sensitivity experiments with showing results for Arctic sea ice extent and sea ice volume in September, and annual global mean temperature in Table 2. There are 5 different pairs of simulations (PI and PD) corresponding to different choice of parameterizations: the original model version (EXP 1: Control), new melt pond parameterization (EXP 2: Melt pond), EXP 2 plus change in fractional snow cover (EXP 3: Melt ponds + snowfrac), EXP 3 plus tuning of wet snow (EXP4: Melt ponds + snowfrac + wet snow), EXP1 + wet snow (EXP5: wet snow). We first note from EXP1 that the estimate of CO_2 needed to have a global annual temperature change around 1 degree was successful, and that this gives decreases of Arctic summer ice extent and ice volume of 18% and 42%, respectively. EXP2 and EXP3 with new melt ponds but without and with the decrease in snow fraction are very similar, and they both show less ice in the PI climate. However, in percent, the changes in extent are very similar to the control experiments, with somewhat smaller decreases in ice volume, Counter-intuitively, the global temperature response in these simulations are also smaller than in the control. This is surprising because increased amount of FYI should give a reduced albedo, and thereby less ice. However, the experiments with lower albedo for melting snow (EXP4 and EXP5) show increased sensitivity. This is seen both in global mean temperature and in the reduction of sea ice. In both experiments, the reduction in sea ice extent is around 30 % and the reduction in sea ice volume near 50 %. These figures are in better agreement with observed estimates (Stroeve et al., 2014; Kwok and Rothrock, 2009; Laxon et al., 2013), but might still be too small, especially when we take into account that the model simulates an equilibrium situation. It is worth noting that EXP4 with the new melt pond parameterization seems less sensitive than EXP5. This is consistent with the results from EXP2 and EXP3.

		Tglob (K)	**NH September ice**	**NH September ice**

			extent (mill km2)	**volume (1000 km3)**
EXP1:	PI	286.17	9.1	24.2
Control	PD	287.17	7.5	14.0
	Differences	**1.00**	**-1.6 (-18%)**	**10.2 (-42%)**
EXP2:	PI+mp	286.22	8.6	19.1
Melt pond	PD+mp	287.10	7.0	12.3
	Differences	**0.88**	**-1.6 (-19 %)**	**-6.8 (-36%)**
EXP3:	PI+mp+hs0	286.40	7.9	16.1
Melt pond +snowfrac	PD+mp+hs0	287.29	6.3	10.3
	Differences	**0.89**	**-1.6 (-20 %)**	**-5.8 (-36 %)**
EXP4 :	PI+mp+hs0+snw	286.44	7.8	14.2
Melt pond + showfrac + wet snow	PD+mp+hs0+snw	287.48	5.6	7.5
	Differences	**1.04**	**-2.2 (-28%)**	**-6.7 (-47%)**
EXP5:	PI+snw	286.23	9.1	23.0
Wet snow	PD+snw	288.30	6.6	11.3
	Differences	**1.07**	**-2.5 (-28%)**	**-11.7 (-51%)**

Table 2: Annual global mean temperature, Northern Hemisphere sea ice extent in September, and Northern Hemisphere sea ice volume in September from different choices of melt pond and snow parameterizations. Pre-industrial results, present day results and their differences are given as PI, PD, Differences, respectively.

1.3.5 Discussion and concluding remarks from melt pond experiments

The present experiments show that climate sensitivity increases somewhat with lower albedo of snow. The effects are relatively small globally, but more important in the Arctic due to the reduction in sea ice. The effects of tuning the snow cover seem more important for the overall simulation than the differences in the parameterizations between FYI and MYI. There are, however, some open questions related to the present simulations with FYI and MYI melt pond distributions. The most important is why all three simulations with the melt pond parameterization included show lower sensitivity with reduced warming, and smaller decrease in sea ice than the experiments with the original formulation? This is unexpected based on the fact that FYI ponds should reduce the overall albedo, and the fact that reduced albedo show a significant increased sensitivity in the wet snow tuning experiment. Until this unexpected behaviour is explained and eventually corrected, we recommended not using the parameterization tested here. Based on the wet snow tuning experiments it seems that a more correct summer melt of ice will increase the modelled Arctic ice sensitivity to be more in line with observations with relatively small impact on the global energy balance. At present it seems more important for the sea ice sensitivity to get the overall melting of snow and ice during summer correct in the 1850 climate simulation than to include changes in melt pond distribution between MYI and FYI.

1.4 Set-up and spin-up of coupled simulation On the basis of the discussion in section 1.2 on results with increased resolution, and the results from section 1.3 on changes in sea ice parameterization, the model version used here is a variation of NorESM1 with 0.9x1.25 resolution in the CAM4-Oslo atmosphere model and the CLM4 land model. Ocean and atmosphere resolution is the same as used in CMIP5, and physical parameterizations used in the models are the same. There are, however, a few adjustments of parameters because of increased horizontal resolution, and also due to the need to improve some aspects of the sea ice simulation. Because of too much snow on Arctic sea ice during summer in the CMIP5 simulations, we have opted to use the decreased wet snow albedo parameters discussed in section 1.3. In addition, because of an unrealistic oscillating wave found in the East Siberian Sea in the CMIP5 model, a parameter which damps coastal or topographic trapped waves have been increased. This later point has a very profound positive impact on regional distribution of Arctic sea ice thickness, as shown later in this section.

A spin-up from a pre-defined ocean initial state should be on the order of 500 years or more. As it was not the purpose of ACCESS task 1.6 to re-do the entire computationally very expensive CMIP5 experiments with higher resolution, the length of this spin-up period should be shortened. In order to do so and still obtain a model system in radiative balance as fast as possible, the spin-up was initialized using the ocean and ice conditions from the first year of the NorESM CMIP5 control simulation. The model had to be re-tuned for the new resolution, but the change in cloud relative humidity thresholds used for the 1 degree resolution version of CCSM4 from NCAR was directly applicable also for NorESM. The NorESM-specific tuning values described in Bentsen et al. (2013) still apply. A new radiative balance was established very fast in the model simulation. The radiative imbalance over the whole spin-up period is 0.06 W m^{-2}, which is well within the CMIP5 requirement. Compared to the CMIP5 control there seems to be larger internal variations in the global temperature field. Figure 4 compares the temperature averages of this spin-up simulation and the CMIP5 control. Note that the initial drop in temperature was not caused by a radiative imbalance, but from a redistribution of heat within the model system. The larger variation may be an effect of the spin-up, however, and not due to model differences. A full spin-up of the entire model system would need on the order of 5000 model years and is not feasible within the given time and resources. Results from the spin-up simulation are also described in ACCESS Newsletter 9.

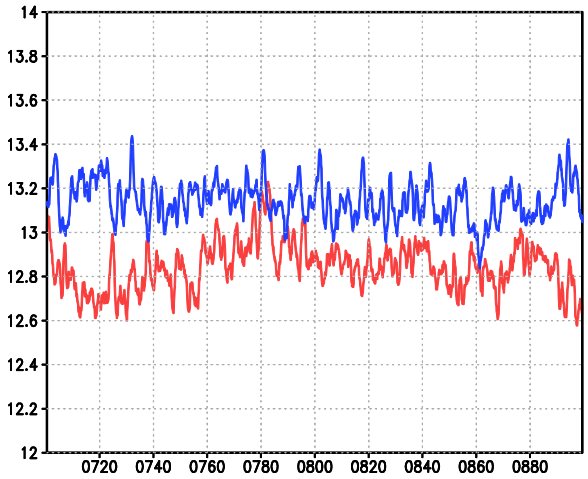

Figure 4: Global average temperature for the ACCESS spin-up (red) and the corresponding period for the CMIP5 control (blue).

1.5 Historical and future scenario, coupled ACCESS version of NorESM.

The spin-up simulation of the ACCESS version of the model was found to produce 0.3 degrees C lower global surface temperature than the CMIP5 version. Since the model was already to cold (Bentsen et al., 2013) this was not ideal, although expected from results with CCSM4. The model is too cold over land, in particular in the tropics as seen in figure 5. There is a slight improvement in root mean square error (rmse), but the general bias pattern is very similar. There is a marked cold bias in SST fields as well, but a promising result is that although SST is colder in general this does not follow from a general reduction but rather from reduced warm biases in particular over the Pacific Ocean. This can also be seen in a reduction of the root mean square error (rmse).

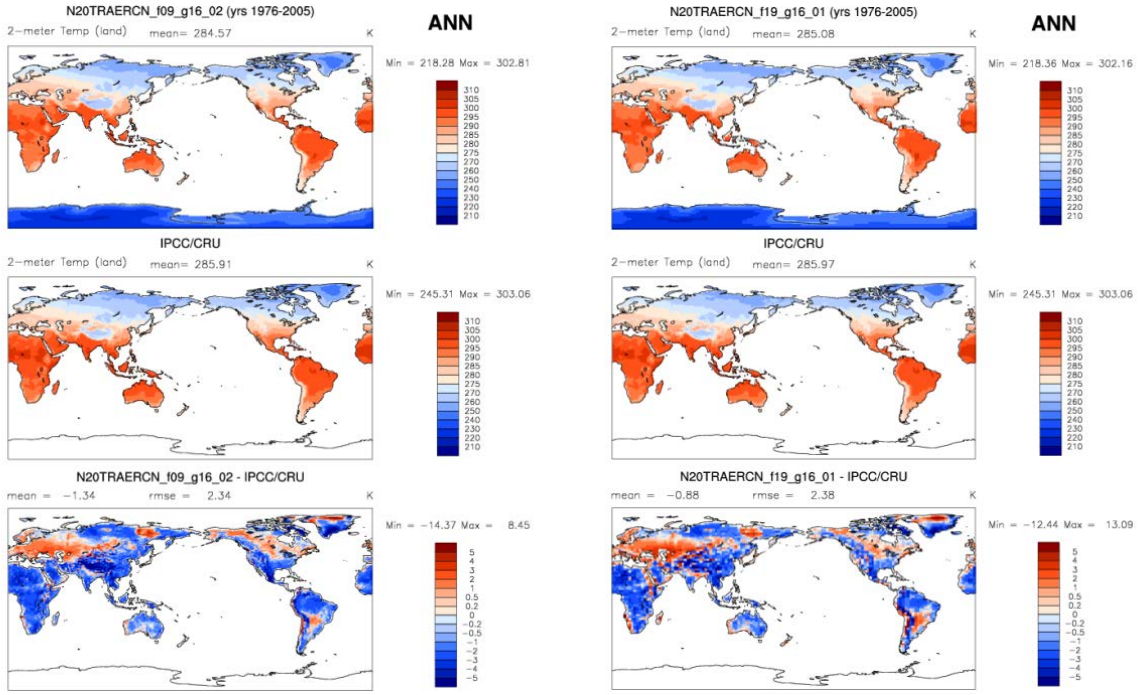

Figure 5: Comparison of modelled and observed 2 meter temperature over land in the ACCESS version (left) and the CMIP5 version (right) of NorESM.

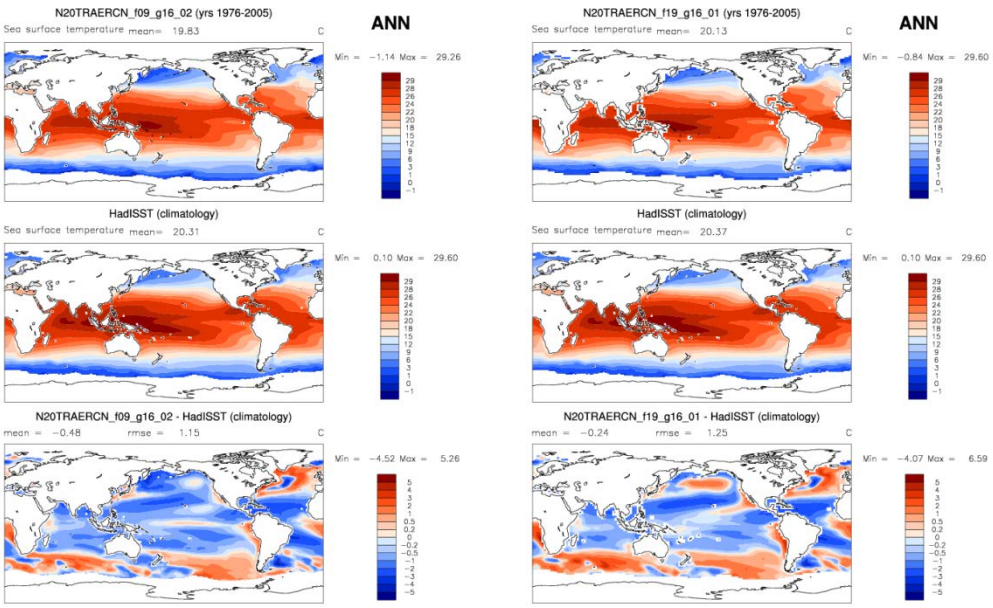

Figure 6: Comparison of modelled and observed SST in the ACCESS (left) and CMIP5 model version (right).

The improvement in SST over the Pacific Ocean did not have much impact on the El Nino signal and is very similar to the CMIP5 version (Figure 7)

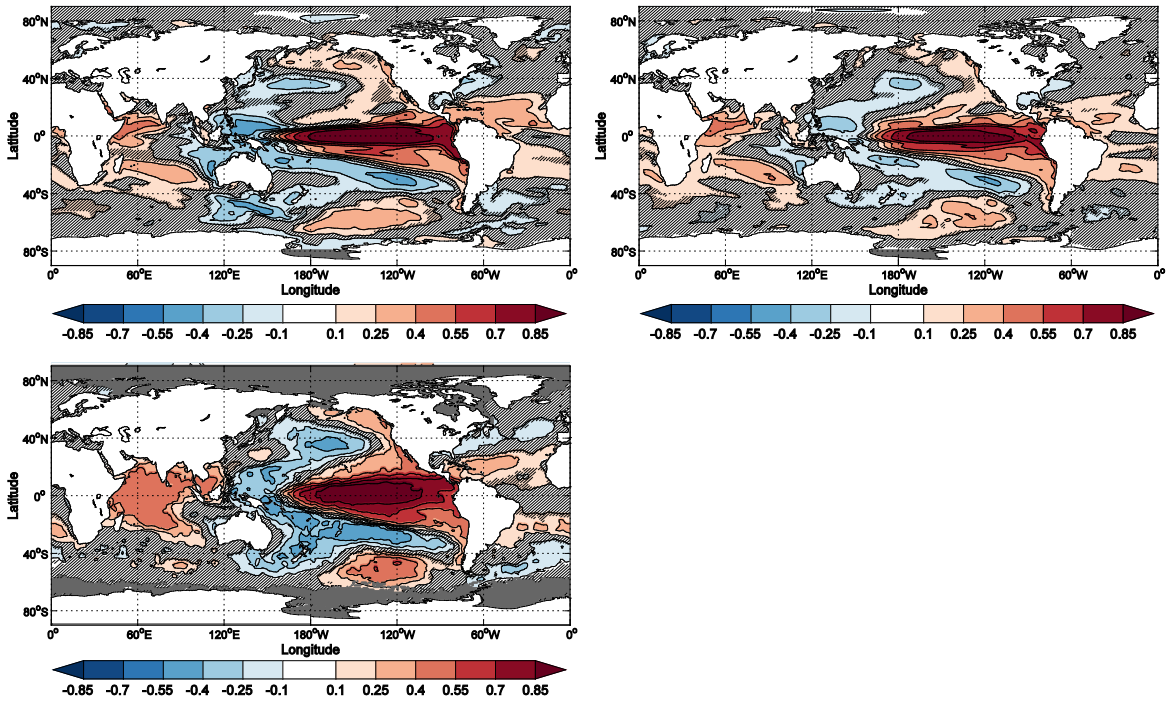

Figure 7: Correlation between local and NINO34 region SST anomalies for the ACCESS version of the model (upper left), CMIP5 (upper right) and HadISST The anomalies are found by subtracting the monthly means for the whole timeseries that span years 1900–2005 for both data sets. Hatched area indicates regions where thecorrelation is not significantly different from vanishing correlation at the 95% confidence level.Same dataset as in figure 18 in Bentsen et al. (2013)

As suspected from the positive SST bias in the Labrador Atlantic Meridional Overturning (AMOC) is still quite high for the ACCESS version even compared to the CMIP5 version (Bentsen et al. 2013;Iversen et al. 2013) but is reduced through the scenario period. (Figure 8)

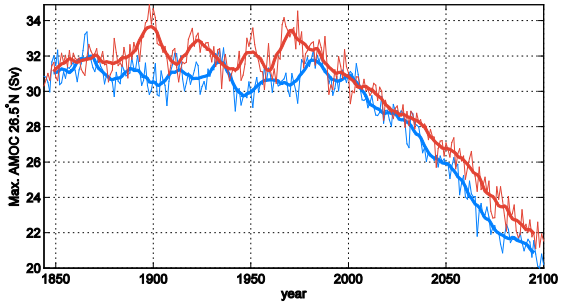

Figure 8: The top panel shows decadal moving averages of the annual max AMOC at 26.5N, where red is the ACCESS version (historic+RCP8.5) and blue are CMIP5 (historic +RCP8.5)

The ACCESS version of NorESM has a slightly higher precipitation rate than the CMIP5 version and compares better with measurements both with regard to bias and RMSE error, although we can not differentiate between circulation and topographical effects. A clear improvement is found in East-Asia where the ACCESS version has a reduced positive bias, despite a general increase in global precipitation. This change is significant on a 95 % level (not shown). Changes in the Arctic are small and in general not significant. Both model versions tend to have a too high precipitation compared to the Legates dataset (Legates and Willmott, 1990) .

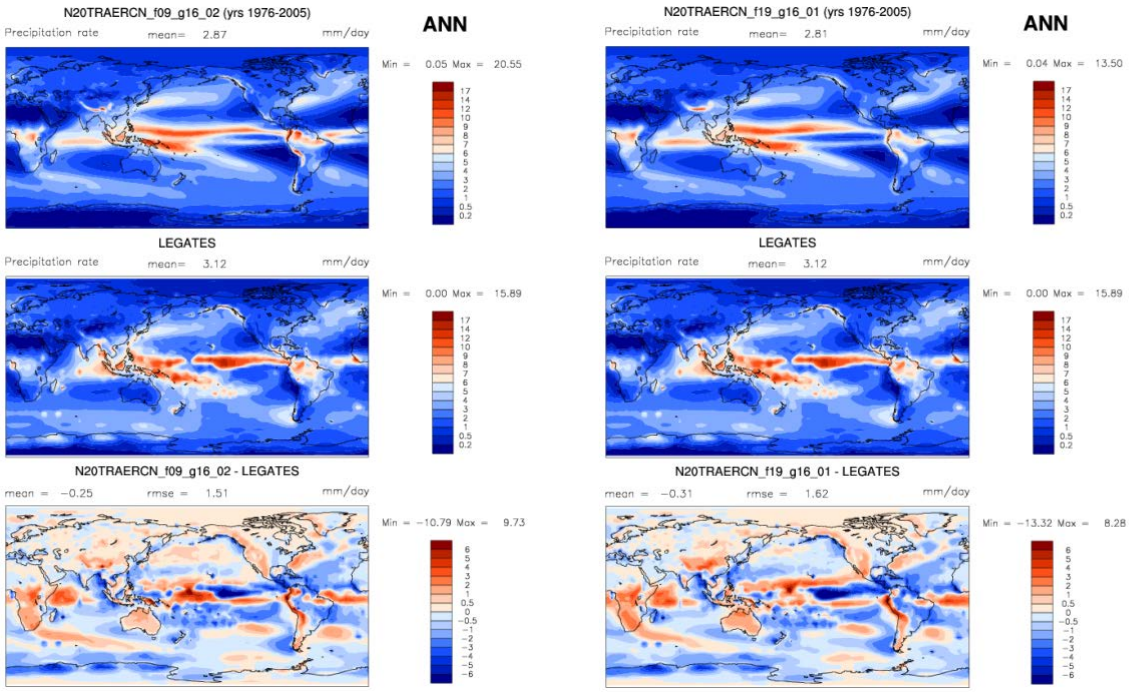

Figure 9: Comparison of modelled and estimated precipitation rate in the ACCESS (left) and the CMIP5 model version (right).

Based on the study by Bitz et al. (2012), which showed that the equilibrium climate sensitivity of CCSM4 increased slightly from 3.13 to 3.20 K by going from 2 to 1 degree atmospheric resolution, we expect only small changes in transient climate, and as seen in Figure 10 the change in model surface temperature from pre-industrial time until today is quite similar (ACCESS version in red). However, the ACCESS version tends to warm more than the CMIP5 version. The additional warming is most pronounced in late 20th century. The difference over the RCP period (2071-2100 minus 1976-2005) between the ACCESS version and the CMIP5 version is negligible (3.08 vs. 3.06 K).

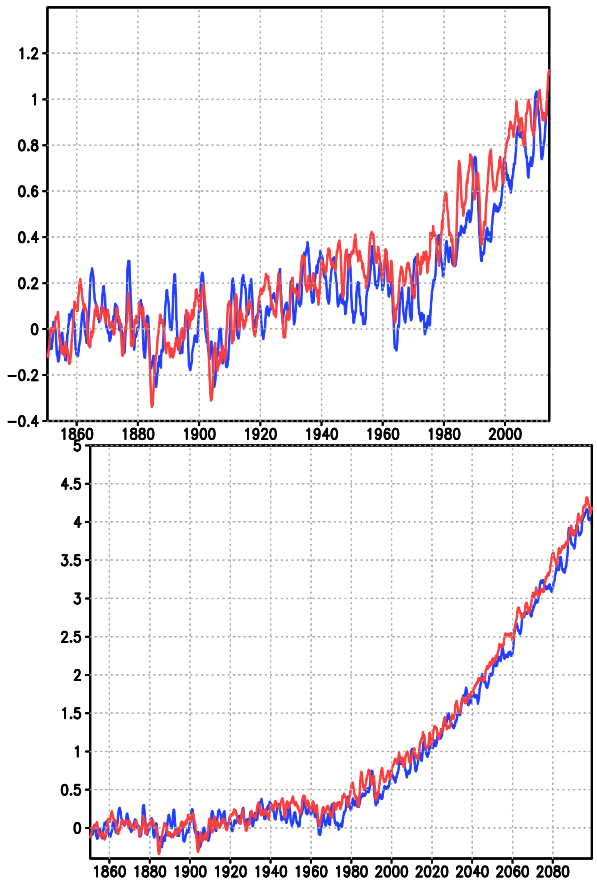

Figure 10: Average model global air temperature at reference height. 1850-2014 on the left, and 1850-2100 from the RCP8.5 scenario on the right. Red is from the ACCESS version of the model. Blue is CMIP5.

As for the simulation of global temperature, the decrease in Arctic sea ice extent is very similar to that found in the CMIP5 version, although the new simulation has a little less ice in the later part of the 20th Century. As seen in Figure 11, this is closer to the observed satellite record, but the overall trend are still smaller than indicated by observations, and more in line with the CMIP5 results.

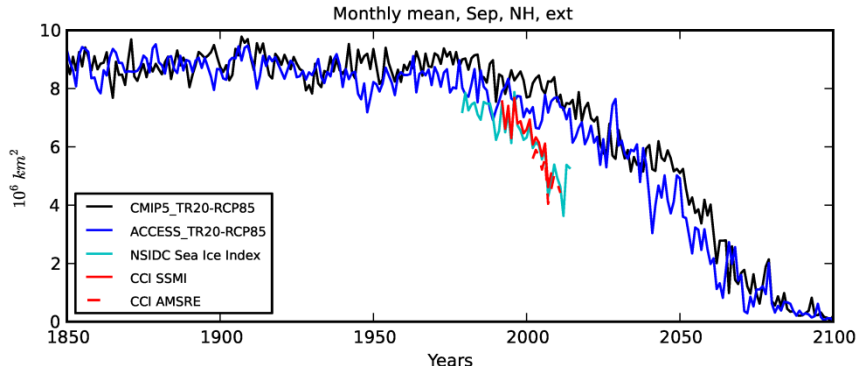

Figure 11: Time evolution of Northern Hemisphere September mean sea ice extent from CMIP5 model and new ACCESS version from 1850-2100, compared with observational estimates from the Sea Ice Index (Fetterer et al 2002, updated through 2014), and from ESA Sea ice Climate Change Initiative (ESA, 2014).

The horizontal distributions of sea ice concentration (SIC) for March and September are shown in Figures 12 and 13 for the Northern and Southern Hemisphere, respectively, and compared with SSM/I data from 1992-2008 from ESA-CCI. The sea ice distributions are very similar to that show by Bentsen et al. (2013) for the CMIP5 version. The winter extent is especially low in the Labrador Sea (Figure 12, left). This is probably a consequence of the strong AMOC circulation in the model, but also the Bering Sea has too little winter ice. During summer (Figure 12, right), the modelled extent is somewhat high in the East Siberian Sea and Laptev Sea, but also in the south-western Beaufort Sea and in the marginal zones of the Barents and Greenland Seas. However, we should note that passive microwave satellite products underestimates SIC in the case of melt ponds. Also the concentration of thin sea ice is underestimated.

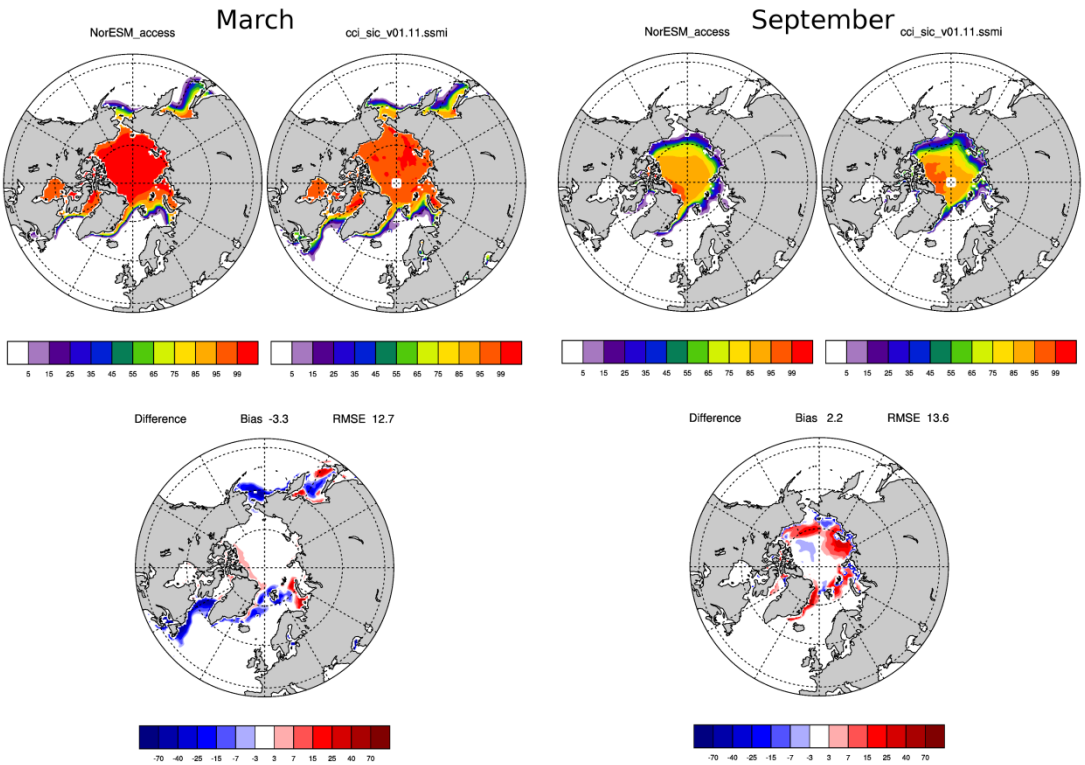

Figure 12: Northern Hemisphere sea ice concentration (SIC) compared with SSM/I based data from 1992-2008 (ESA CCI, 2014).

The overall distribution of Southern Hemisphere (SH) SIC compares well with the observations, and this is similar to that found in the CMIP5 version. The extent is somewhat larger than indicated by observations, while the area mean concentration is very similar. In general, the simulation of the SH sea ice is very similar to the CMIP5 results.

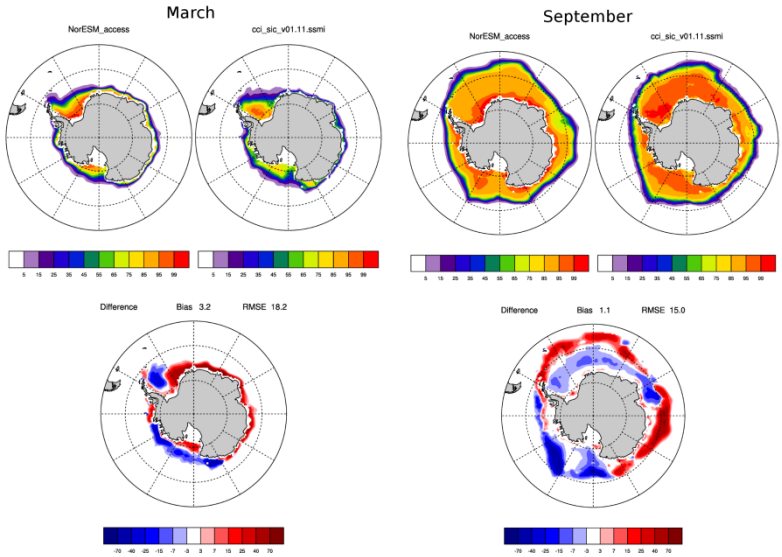

Figure 13: Similar to Figure 12 for the Southern Hemisphere.

NH sea ice thickness (SIT) is an important variable, both for navigation and marine operations in the Arctic, but also for the vulnerability of the sea ice to summer melt. Thin ice can more easily melt during summer than thick ice, which more easily will survive the summer and become multiyear ice. To get a realistic sensitivity of the sea ice to warmer temperature, it is very important to have a reasonable ice thickness distribution. The present ACCESS simulations have very much better regional distribution of SIT in the Arctic compared with the CMIP5 version. This is clearly seen in Figure 14 showing late autumn SIT from the ACCESS run (upper left), CMIP5 (upper right) and ICESat observations (below) (Kwok et al. 2009) for the period 2003-2007. Although this satellite record is very short, it clearly shows the large improvement of the regional SIT distribution between the two model versions. The improvements are largest near the New Siberian Islands and in the East Siberian Sea. This is the region where the CMIP5 model had spurious variability in the sea surface height (some sort of trapped waves), which generated excessive convergence and divergence in the ice cover with the consequence of large generation of open water that could refreeze. In addition there was massive ridging of ice. Increased damping of these waves in the ocean model made the simulation much more realistic in this region. Furthermore, although less important, small changes in the wind field and general circulation in the 1 degree version of the atmosphere model contributed to the improvement of SIT regional distribution. Still, however, the model simulation seems to give too thick ice for this period.

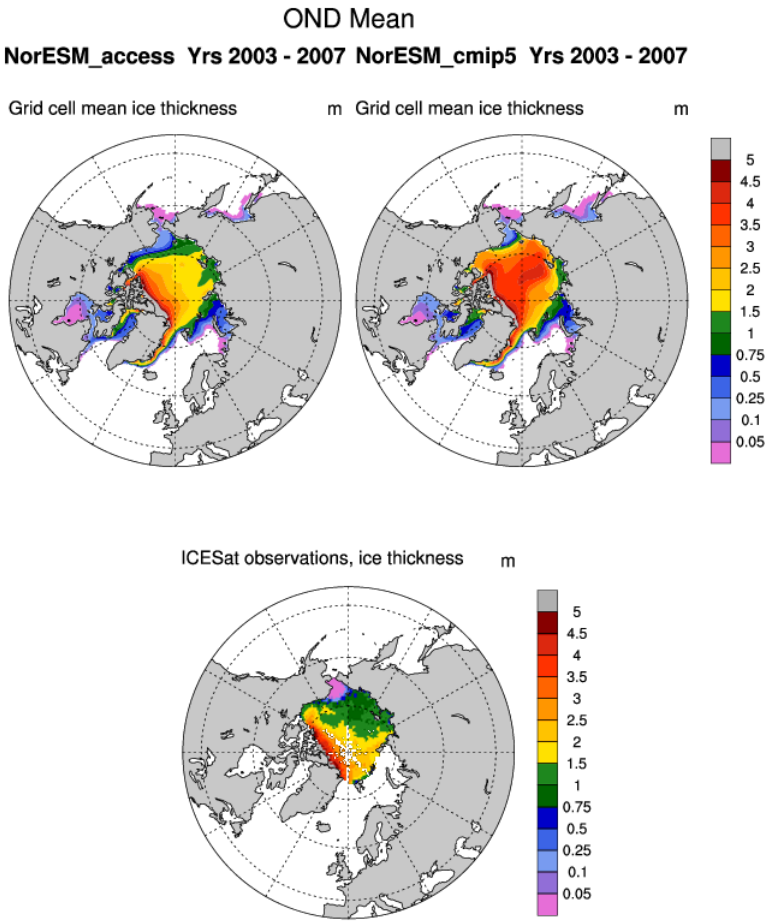

Figure 14: Sea ice thickness distribution compared with ICEsat satellite data.

To look closer at the time evolution of the SIT, the simulations are compared with upward looking sonar (ULS) data for moored platforms at the North Pole (NP) and submarine ULS data (Lindsay, 2013). Figure 15 shows the seasonal cycle of sea ice draft (depth below sea level) from the NorESM CMIP5 historic ensemble and from the ACCESS simulation together with ULS data from an approximately 100x100 square km region around the NP. The data are grouped into the time periods 1975-1984, 1984-1994, 1995-2004 and 2005-2009. It is clear from both observations and models that the draft decrease from the first to the last period. For 1975-1984, the CMIP5 version seems closest to the winter draft, while the ACCESS version is closest to the summer draft. Both models underestimate the amplitude of the seasonal cycle with too little melting during summer and too little freezing during winter. For the two last periods the draft reduces considerably, and here the ACCESS version is closest to observations width winter draft very close to the observed values, but still too thick ice during late summer.

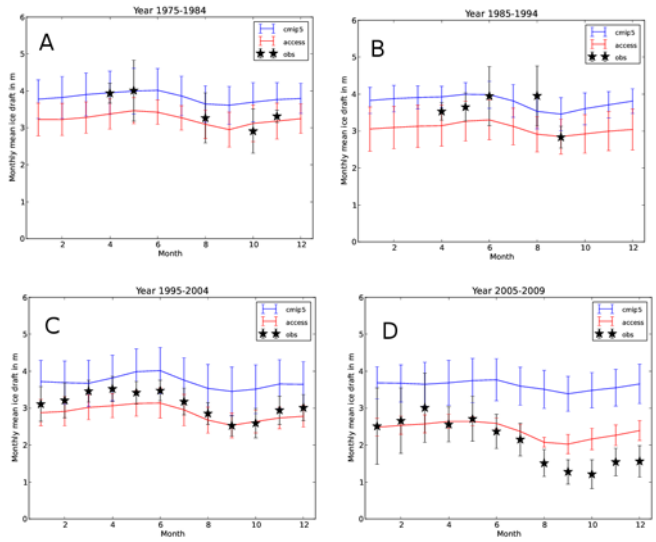

Figure 15: Seasonal cycle of sea ice draft near the North Pole from the NorESM historic CMIP5 ensemble (blue) and the ACCESS simulation (red) compared with upward looking sonar data (stars) (Lindsay, 2013).

The SIC and SIT together defines the sea ice volume, and as this is an integrated estimate sea ice mass it also gives a measure of the energy needed to melt all the sea ice. Sea ice volume tells much more about the state of the sea ice than the much simpler sea ice extent shown earlier. Figure 16 shows the time evolution of sea ice volume for the CMIP5 and ACCESS simulations. As for global temperature and sea ice extent, the evolutions of the model simulations are very similar, but the ACCESS version has somewhat less ice. The trend in September sea ice volume in the period 1979-2011 is -3.1 1000 km^3/decade, very similar to -3.2 1000 km^3/decade found in the Pan-Arctic Ice-Ocean Modelling and Assimilation system (PIOMAS, Zhang and Rothrock, 2003; Schweiger et al, 2011). See http://psc.apl.uw.edu/research/projects/arctic-sea-ice-volume-anomaly/ for and update time series of the PIOMAS volume analysis.

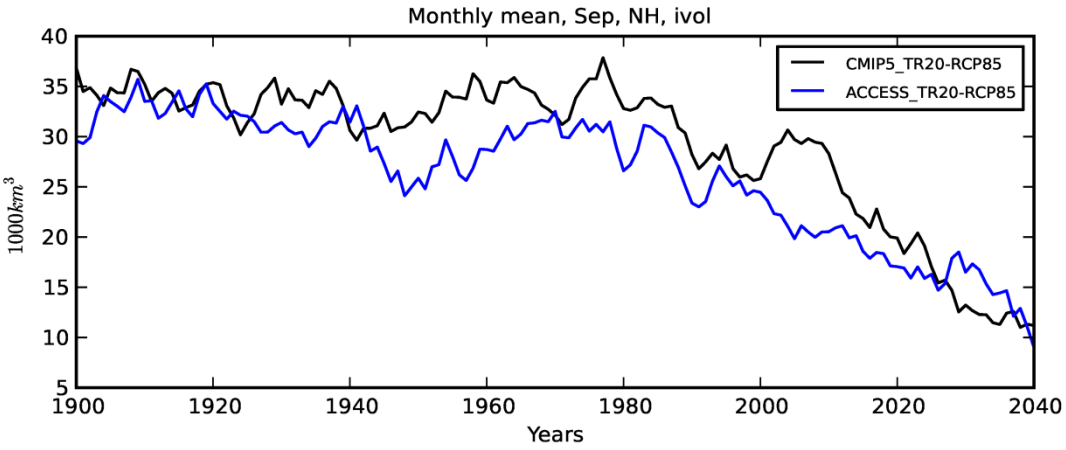

Figure 16: Figure 16: Evolution of sea ice volume from the CMIP5 and ACCESS simulations.

Although NorESM has larger sea ice volume in the Arctic than PIOMAS, the downward trends are very similar; implying that the amount of energy used to melt sea ice is also comparable. The NorESM simulations show similar downward trends in volume through the coming decades and there are no significant difference between the two simulations in this respect.

1.6 Summary

The Arctic plays a key role in the climate system. During winter darkness it produces major cooling of the earth's atmosphere and entire climate system, and changes in the contents of climate gases (including water vapour) strongly influences the vertical profile of the cooling and thus the realized surface temperature. Together with the net heating of the tropics, the Arctic cooling determines the strength of the mid-latitude jets and the speed and strength of the extra-tropical cyclones, as well as exerting forcing of ocean currents and deep water formation. During summer the solar radiation changes this major cooling property of the Arctic, although the high albedo of sea-ice and remaining snow and ice on land is an important regulator of absorbed solar radiation.

In this connection, important properties of the Arctic region itself include the extent, thickness, and structure of the sea-ice and snow. Furthermore, the absorption of sunlight by soot aerosols is particularly important in the Arctic with its natural high-albedo surface. Finally, the efficiency of and manner that the low-latitude heat-excess is transported into the Arctic will both influence and be a consequence of the realized latitudinal temperature contrasts.

Therefore, both climate variability and the climate response to forcing are particularly large in the Arctic, in consequence of the complex interactions between processes in the region and teleconnections. The work with NorESM for ACCESS has addressed the three issues in great depth, because they are relevant for any earth system or global climate model. The work on black carbon and soot pertaining to the Arctic, clearly demonstrates the complex links between soot, Arctic sea-ice, and meridional heat transport, as well as emphasizing that emissions in the Arctic are much more prone to influence the climate. These results are relevant for all modelling work addressing climate and climate change in general and in the Arctic on particular.

Most state-of-the-art global climate models and ESMs show systematic errors in representing North-Atlantic storm-tracks and blocking (Dawson et al. 2012; Zappa et al. 2013). This is also true for NorESM applied for CMIP5, and since experiments like Jung et al. (2012) indicate that spatial resolution is a major limiting factor for this, we used NorESM for investigating this. Although we find improvements for higher resolution, this single element does not appear to be entirely sufficient for all seasons.

Both increasing the resolution and upgrading the modelled albedo of snow on sea-ice, significantly improved the Arctic regional distribution of sea ice thickness and precipitation. We also investigated the sensitivity of Arctic sea ice to the different distribution of melt ponds on first-year and multi-year sea ice. These investigations were non-conclusive with respect to the question if these differences are important for the climate sensitivity. It seems more important to have a realistic melting of snow on sea ice in our model.

The data for the historical period and RCP8.5 scenario with the ACCESS version of NorESM are stored and can be made available for people who want to study the changes further.

These experiments and their results are mainly relevant for model studies of climate. The work done in ACCESS has been an important for getting experience with increased resolution and different parameterisations that are relevant for the next version of NorESM.The resolution experiment is also relevant for numerical weather prediction, although NWP-models already employs models with much higher resolution at present. The work on sea-ice is probably mainly relevant for NWP in the extended range beyond 10 days.

Acknowledgements: In addition to support from the EC's 7th framework program via the ACCESS project, this work has been supported by the Research Council of Norway through the Notur/NorStore programmes for heavy computing and storage. Large parts of the NorESM has been provided by NCAR / DOE CESM programme.

2 References

Bentsen, M., I. Bethke, J. B. Debernard, T. Iversen, A. Kirkevåg, Ø. Seland, H. Drange, C. Roelandt, I. A. Seierstad, C. Hoose, and J. E. Kristjánsson: The Norwegian Earth System Model, NorESM1-M. Part 1: Description and basic evaluation, Geosci. Model Dev., 6, 687-720, doi:10.5194/gmd-6-687-2013.

Bitz, C.M., K.M. Shell, P.R. Gent, D.A. Bailey, G. Danabasoglu, K.C. Armour, M. Holland, and J.T. Kiehl, 2012: Climate sensitivity of the Community Climate System Model, version 4. J. Clim., **25**, 3053–3070, DOI: 10.1175/JCLI-D-11-00290.1

Bjerknes, J. (1969): Atmospheric Teleconnections from The Equatorial Pacific. *Mon. Wea. Rev.*, **97**, 163–172

Brandt, R. E., Stephen G. Warren, Anthony P. Worby, and Thomas C. Grenfell, 2005: Surface Albedo of the Antarctic Sea Ice Zone. J. Climate, **18**, 3606–3622. doi:http://dx.doi.org/10.1175/JCLI3489.1

Corti, S., Molteni, F., & Palmer, T. N. (1999). Signature of recent climate change in frequencies of natural atmospheric circulation regimes. *Nature*, *398*(6730), 799-802.

Dawson, A., Palmer, T. N., & Corti, S. (2012). Simulating regime structures in weather and climate prediction models. *Geophysical Research Letters*, *39*(21).

Deser, C., Phillips, A. S., Alexander, M. A., & Smoliak, B. V. (2014). Projecting North American Climate over the Next 50 Years: Uncertainty due to Internal Variability*. *Journal of Climate*, *27*(6), 2271-2296.

Fetterer, F., K. Knowles, W. Meier, and M. Savoie. 2002, updated daily. *Sea Ice Index*. Boulder, Colorado USA: National Snow and Ice Data Center. Digital media.

ESA (2014) ESA CCI Sea Ice: Ice concentration from SSMI, 1992-2008, Available from Arctic Data Centre (http://arcticdata.met.no)

Holland, M. M., D. A. Bailey, B. P. Briegleb, B. Light, and E. Hunke (2012), Improved sea ice shortwave radiation physics in CCSM4: The impact of melt ponds and aerosols on Arctic sea ice, J. Clim., 25(5), 1413–1430, doi:10.1175/JCLI-D-11-00078.1

Hoskins, B. J. and Karoly D. J., (1981). The Steady Linear Response of a Spherical Atmosphere to Thermal and Orographic Forcing. *J. Atmos. Sci.*, **38**, 1179., doi:10.1175/1520-0469(1981).

Iversen, T., M. Bentsen, I. Bethke, J. B. Debernard, A. Kirkevåg,, Ø. Seland, H. Drange, J. E. Kristjansson, I. Medhaug, M. Sand, and I. A. Seierstad: The Norwegian Earth System Model, NorESM1-M - Part 2: Climate response and scenario projections, Geosci. Model Dev., 6, 389-415, doi:10.5194/gmd-6-389-2013, 2013.

Jiao, C., M. G. Flanner, Y. Balkanski, S. E. Bauer, N. Bellouin, T. Berntsen, H. Bian, K. Carslaw, M. Chin, N. De Luca, T. Diehl, S. Ghan, T. Iversen, A. Kirkevåg, D. Koch, X. Liu, J. E. Penner, G. Pitari, M. Schulz, Ø Seland, R. B. Skeie, S. D. Steenrod, P. Stier, T. Takemura, K. Tsigaridis, T. van Noije, Y. Yun, and K. Zhang: An AeroCom assessment of black carbon in Arctic snow and sea ice, Atmos. Chem. Phys. Discuss., 13, 26217-26267, doi:10.5194/acpd-13-26217-2013. (Accepted for ACP on February 5'th, 2014).

Jung, T., M.J. Miller, T.N. Palmer, P. Towers, N. Wedi, D. Achuthavarier, J. M. Adams, E. L. Altshuler, B. A. Cash, J. L. Kinter III, L. Marx, and C. Stan, and K. I. Hodges: High-Resolution Global Climate Simulations with the ECMWF Model in Project Athena: Experimental Design, Model Climate, and Seasonal Forecast Skill. *J. Climate*, **25**, 3155–3172. doi: http://dx.doi.org/10.1175/JCLI-D-11-00265.1. 2012.

Kirkevåg, A., T. Iversen, Ø. Seland, C. Hoose, J. E. Kristjánsson, H. Struthers, A. Ekman, S. Ghan, J. Griesfeller, D. Nilsson, and M. Schulz: Aerosol-climate interactions in the Norwegian Earth System Model - NorESM1-M, Geosci. Model Dev., 6, 207-244, doi:10.5194/gmd-6-207-2013, 2013.

Kwok, R., and D. A. Rothrock (2009), Decline in Arctic sea ice thickness from submarine and ICESat records: 1958–2008, Geophys. Res. Lett., 36, L15501, doi:10.1029/2009GL039035

Laxon S. W., K. A. Giles, A. L. Ridout, D. J. Wingham, R. Willatt, R. Cullen, R. Kwok, A. Schweiger, J. Zhang, C. Haas, S. Hendricks, R. Krishfield, N. Kurtz, S. Farrell and M. Davidson (2013), CryoSat-2 estimates of Arctic sea ice thickness and volume, Geophys. Res. Lett., 40, 732–737, doi:10.1002/grl.50193

Legates, D.R. and C.J. Willmott, 1990.Mean seasonal and spatial variability in gauge-corrected, global precipitation. Int. J. Climatology, 10, 111-127.

Lindsay, R. W. 2013. Unified Sea Ice Thickness Climate Data Record, 1975-2012. Boulder, Colorado USA: National Snow and Ice Data Center. http://dx.doi.org/10.7265/N5D50JXV

Kwok, R., G. F. Cunningham, M. Wensnahan, I. Rigor, H. J. Zwally, and D. Yi (2009), Thinning and volume loss of the Arctic Ocean sea ice cover: 2003–2008, J. Geophys. Res., 114, C07005, doi:10.1029/2009JC005312

Mauritzen, C., E. Hansen, M. Andersson, B. Berx, A. Beszczynska-Möller, I. Burud, K.H. Christensen, J. Debernard, L. de Steur, P. Dodd, S. Gerland, Ø. Godøy, B. Hansen, S. Hudson, F. Høydalsvik, R. Ingvaldsen, P.E. Isachsen, Y. Kasajima, I. Koszalka, K.M. Kovacs, M. Køltzow, J. LaCasce, C.M. Lee, T. Lavergne, C. Lydersen, M. Nicolaus, F. Nilsen, O.A. Nøst, K.A. Orvik, M. Reigstad, H. Schyberg, L. Seuthe, Ø. Skagseth, J. Skarðhamar, R. Skogseth, A. Sperrevik, C. Svensen, H. Søiland, S.H. Teigen, V. Tverberg, C. Wexels Riser (2011), Closing the Loop – Approaches to monitoring the state of the Arctic Mediterranean during the International Polar Year 2007–2008, Progress in Oceanography, bf 90, pp. 62–89, doi:10.1016/j.pocean.2011.02.010

Myhre, G., Samset, B. H., Schulz, M., Balkanski, Y., Bauer, S., Berntsen, T. K., Bian, H., Bellouin, N., Chin, M., Diehl, T., Easter, R. C., Feichter, J., Ghan, S. J., Hauglustaine, D., Iversen, T., Kinne, S., Kirkevåg, A., Lamarque, J.-F., Lin, G., Liu, X., Lund, M. T., Luo, G., Ma, X., van Noije, T., Penner, J. E., Rasch, P. J., Ruiz, A., Seland, Ø., Skeie, R. B., Stier, P., Takemura, T., Tsigaridis, K., Wang, P., Wang, Z., Xu, L., Yu, H., Yu, F., Yoon, J.-H., Zhang, K., Zhang, H., and Zhou, C.: Radiative forcing of the direct aerosol effect from AeroCom Phase II simulations, Atmos. Chem. Phys., 13, 1853-1877, doi:10.5194/acp-13-1853-2013, 2013.

Palmer, T. N. (1999) A nonlinear dynamical perspective on climate prediction. *J. Clim.* **12**, 575–591 (1999)

Pedersen, C. A., E. Roeckner, . Lüthje, and J.-G. Winther (2009), A new sea ice albedo scheme including melt ponds for ECHAM5 general circulation model, J. Geophys. Res., 114, D08101, doi:10.1029/2008JD010440

Polashenski, C., D. Perovich, and Z. Courville (2012), The mechanisms of sea ice melt pond formation and evolution, J. Geophys. Res., 117, C01001, doi:10.1029/2011JC007231

Samset, B. H., G. Myhre, M. Schulz, Y. Balkanski, S. Bauer, T. K. Berntsen, H. Bian, N. Bellouin, T. Diehl, R. C. Easter, S. J. Ghan, T. Iversen, S. Kinne, A. Kirkevåg, J.-F. Lamarque, G. Lin, X. Liu, J. Penner, Ø. Seland, R. B. Skeie, P. Stier, T. Takemura, K. Tsigaridis, K. Zhang (2012): Black carbon vertical profiles strongly affect its radiative forcing uncertainty, Atmos. Chem. Phys., 13, 2423-2434, doi:10.5194/acp-13-2423-2013, 2013.

Sand, M., T. K. Berntsen, J. E. Kay, J. F. Lamarque, Ø. Seland, and A. Kirkevåg (2013a), The Arctic response to remote and local forcing of black carbon, Atm. Chem. Phys., 13, 211-224, doi:10.5194/acp-13-211-2013, 2013.

Sand, M., T. K. Berntsen, Ø. Seland, and J. E. Kristjánsson (2013b), Arctic surface temperature change to emissions of black carbon within Arctic or midlatitudes, J. Geophys. Res. Atmos., 118, 7788–7798, doi:10.1002/jgrd.50613.

Sand, M., Iversen, T., Bohlinger, P., Kirkevåg, A., Seierstad, I. A., Seland, Ø., and Sorteberg, A., (2015), A standardized global climate model study showing unique properties for the climate response to black carbon aerosols. Accepted, Journal of Climate http://dx.doi.org/10.1175/JCLI-D-14-00050.1

Schweiger, A., R. Lindsay, J. Zhang, M. Steele, H. Stern, and R. Kwok (2011), Uncertainty in modeled Arctic sea ice volume, J. Geophys. Res., 116, C00D06, doi:10.1029/2011JC007084

Seland Ø., and Debernard, J. Sensitivities of Arctic Sea-ice in Climate Modelling (2014) ACCESS Newsletter 9.

Stroeve, J., L. C. Hamilton, C. M. Bitz, and E. Blanchard-Wrigglesworth (2014), Predicting September sea ice: Ensemble skill of the SEARCH Sea Ice Outlook 2008–2013, Geophys. Res. Lett., 41, 2411–2418, doi:10.1002/2014GL059388

Zappa, G. G., L. C. Shaffrey, and K. I. Hodges, 2013: The Ability of CMIP5 Models to Simulate North Atlantic Extratropical Cyclones*. *J. Climate*, **26**, 5379–5396. doi: http://dx.doi.org/10.1175/JCLI-D-12-00501.1

Zhang, J. and D. A. Rothrock, 2003: Modeling Global Sea Ice with a Thickness and Enthalpy Distribution Model in Generalized Curvilinear Coordinates. *Mon. Wea. Rev.*, **131**, 845–861. doi: http://dx.doi.org/10.1175/1520-0493(2003)131<0845:MGSIWA>2.0.CO;2